

## Photoemission Spectroscopic Studies on Oxide/SiC Interfaces Formed by Dry and Pyrogenic Oxidation

Y. Hijikata<sup>1</sup>, H. Yaguchi<sup>1</sup>, Y. Ishida<sup>2</sup>, M. Yoshikawa<sup>3</sup>, T. Kamiya<sup>3</sup>  
and S. Yoshida<sup>1</sup>

<sup>1</sup>Department of Electrical and Electronic Systems Engineering, Saitama University, 255 Shimo-Okubo, Sakura-ku, Saitama-shi, Saitama 338-8570, Japan

<sup>2</sup> National Institute of Advanced Industrial Science and Technology, Japan

<sup>3</sup> Japan Atomic Research Institute Takasaki, Japan

**Keywords:** photoelectron spectroscopy, pyrogenic oxidation, Ar post-oxidation annealing, oxide/SiC interface, bonding, band lineup, capacitance to voltage measurement

**Abstract.** The difference in the structure of oxide/SiC interface between dry and pyrogenic oxidation and the effect of post-oxidation annealing in Ar atmosphere on the interfaces have been studied by X-ray and ultraviolet photoelectron spectroscopy to make clear the interface structures which spoil the electrical properties. It is found that intermediate layers containing Si<sup>1+</sup> oxidation states exist in both cases of oxidation method and the thickness of the layer changes by Ar annealing. It is also found that the oxide/SiC band offsets and the structures of O2p peak, observed in valence band spectra, change remarkably by Ar POA in both cases of oxidation method. The bond states at SiC/oxide interfaces have been discussed by considering these results together with the results from C-V measurements.

### Introduction

SiC MOSFETs have severe problems to be solved before practical use, such as their higher on-resistances than those predicted from bulk properties of SiC. It has been reported that the reason for this poor electrical property is due to the low channel mobility  $\mu_{ch}$  in inversion layers of SiC MOSFETs,[1] and the small  $\mu_{ch}$  results from the high interface state density  $D_{it}$ . [2] It is well known that the electrical properties of SiC MOS capacitors and MOSFETs depend strongly on the oxidation methods and post-oxidation processes.[3] A lot of photoemission spectroscopic studies have been carried out to make clear the structure of oxide/SiC interfaces.[4,5] We have reported from the results of x-ray photoelectron spectroscopy (XPS) measurements for slope shaped oxide films with various post-oxidation processes that several differences in photoemission peaks were observed.[6,7] However, so far, nothing can be specified as the origins which bring about poor electrical property such as high  $D_{it}$ . In our recent work,[8] it was found from the results of capacitance to gate-bias voltage (C-V) measurements that the flat-band voltage  $V_{fb}$  shifts toward higher gate-bias voltage side with increasing the sweep range of gate-bias voltage in the accumulation side, only when the oxidation is carried out under high purity oxygen flow. Besides, the magnitude of this shift, denoted as  $\Delta V_{fb}^{dyn}$ , decreases by post-oxidation annealing (POA) at the temperatures higher than 600 °C. Since the large  $\Delta V_{fb}^{dyn}$  should also be a severe problem for the practical use of SiC MOS device, it is important to specify the interface structure which brings about the large  $\Delta V_{fb}^{dyn}$ .

In this report, the difference of oxide/SiC interface structures between dry and pyrogenic oxidation and the effect of post-oxidation annealing in Ar atmosphere (Ar POA) for the interfaces have been studied by X-ray and ultraviolet photoelectron spectroscopy (XPS and UPS) to make clear the interface structures which bring about the change of electrical properties. Also, the oxide/SiC band lineups were determined by the analysis of O1s energy loss spectra and the valence band spectra. We will discuss the interface structures and the band structures by considering the results of XPS and UPS together with those of C-V measurements for the samples oxidized by the same processes as were done for XPS and UPS.

## Experiments

Epitaxial wafers of 4H-SiC with  $8^\circ$  off-oriented (0001) Si-face, *n*-type,  $N_d - N_a = 6 \times 10^{15} \text{ cm}^{-3}$  were used and four kinds of specimens were prepared in this study. After standard RCA cleaning, two specimens were oxidized up to around 50 nm in oxide thickness in pure dry  $\text{O}_2$  flow at  $1200^\circ\text{C}$  (denoted as sample (a) and sample (b)), and the other two specimens were oxidized up to the same thickness as samples (a) and (b) in mixed  $\text{O}_2$  and  $\text{H}_2$  flow ( $\text{O}_2:\text{H}_2 = 3:1$ ) at  $1200^\circ\text{C}$  (denoted as sample (c) and sample (d)). The samples (a) and (c) were quenched at room temperature after oxidation. The samples (b) and (d) were followed by annealing in Ar atmosphere for 3 hours at  $950^\circ\text{C}$ . All the samples were etched off by buffered HF solution, resulting in the oxide thickness of  $\sim 1.3 \text{ nm}$ , measured by a spectroscopic ellipsometer. XPS and UPS measurements were performed with non-monochromatized Mg  $K\alpha$  line ( $=1253.6 \text{ eV}$ ) and He II line ( $=40.8 \text{ eV}$ ) as a light source, respectively.

## Results and Discussions

The XPS spectra in Si2p and C1s regions for samples (a)-(d) are shown in Figs. 1-i) and ii), respectively. The horizontal axes were calibrated by referring the SiC peak in C1s region (its binding energy  $= 282.7 \text{ eV}$ ), and the spectra were normalized by the corresponding SiC peak intensity of C1s. All the measured spectra were decomposed by Gaussian, taking into account Lorentzian contribution as well, as reported in Ref. [5]. Figures 1-iii) and iv) show the deconvolution results for sample (a) at  $\theta_e = 90^\circ$ , for example. Here, in-take angle of photoelectron is indicated by  $\theta_e$ , which is regarded as an angle from the sample surface. Only the peaks corresponding to  $\text{Si}^{1+}$  oxidation state and C-H bond in Si2p and C1s, respectively, were observed except those from Si-C bonds. The features of the spectra for samples (b)-(d) were similar to that for sample (a). The C-H peak observed is thought to be due to surface contamination because the C-H peak intensity increases with increasing the surface sensitivity of measurements, *i.e.* with decreasing  $\theta_e$ . Therefore, only the peak corresponding to  $\text{Si}^{1+}$  oxidation

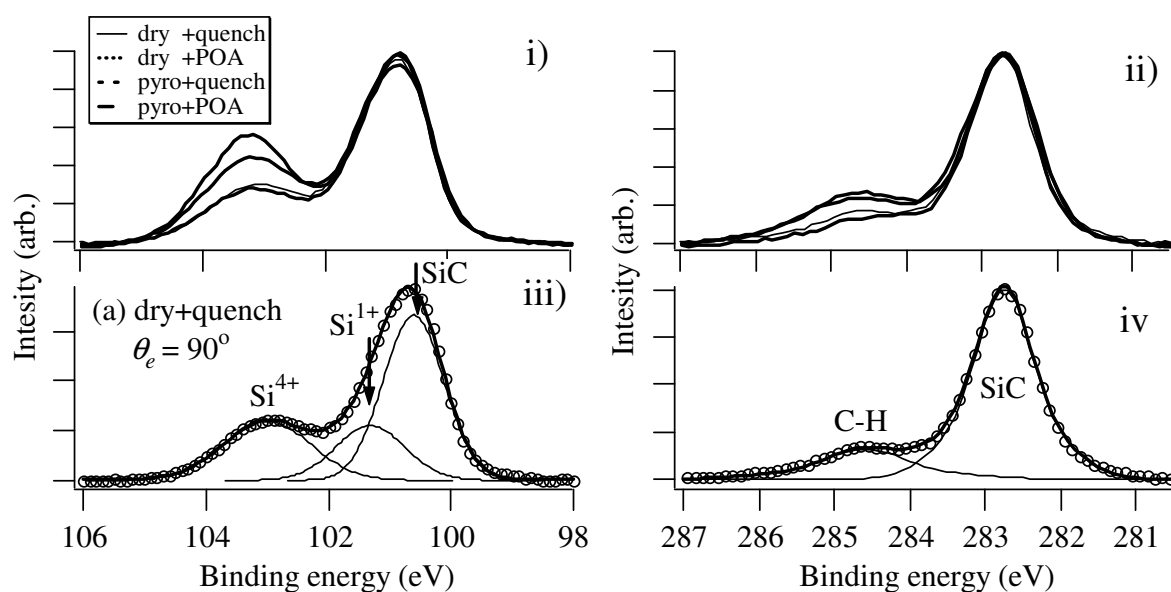


Fig. 1. XPS spectra of the samples (a)-(d): i) Si2p at  $\theta_e=90^\circ$ , ii) C1s at  $\theta_e=90^\circ$ , iii) deconvolution of Si2p for sample (a), iv) deconvolution of C1s for sample (a).

state is observed at the interface. The  $\text{Si}^{1+}$  state is considered to be due to the existence of C-Si\*-O-Si bonds parallel to *c*-axis, where asterisk denoted as a Si termination layer in SiC bulk crystal. The intensity ratio  $\text{Si}^{1+}/\text{Si}^{0+}$  for samples (a)-(d) are listed in Tab. 1, where  $\theta_e$  is selected for each sample so

as to cancel out the difference in oxide thickness between the samples. We found that the value of  $\text{Si}^{1+}/\text{Si}^{0+}$  decreases by Ar POA in the case of dry oxidation, while the value increases by Ar POA in the case of pyrogenic oxidation.

Figure 2 shows the O1s energy loss spectra for samples (a)-(d). The energy gaps  $E_g$  of interface layers were determined by the scheme reported in Ref. [9], as also shown in Tab. 1. The value of  $E_g$  for pyrogenic oxidation is larger than that for dry oxidation in both cases of quenched and Ar POA samples, and the values increased by Ar POA in both cases of oxidation method.

The UPS spectra for samples (a)-(d) at various  $\theta_c$  are shown in Fig. 3. We can see two peaks in the spectra, large one around 5.5 eV and one at the higher energy side ( $\sim 9.5$  eV). It is considered that this twin peak is originated from O2p, as reported in the case of oxide films on Si that the twin peak with the peaks at 7.0 and 10.5 eV below Si valence band maximum (VBM) arises in O2p region when the oxide thickness is around or less than 10 nm.[10] It has been also reported in ref.[10] that the peak at lower energy side and that at higher energy side of the O2p twin peak correspond to O2p non-bonding state and intermediate oxidation state, respectively. It is found from the figure that the intensity of the O2p twin peak decreases by Ar POA. This decrease can be explained by the reduction in the number of oxygen atoms at the interface. On the other hand, the difference in O2p peak intensities between two oxidation methods is observed in POA samples, but not in quenched samples. These results can be explained by the enhancement of oxygen removing in aid of hydrogen. Figure 3 shows that the changes of O2p intensity by Ar POA for both the oxidation methods become larger with decreasing  $\theta_c$ . This suggests that the change of the interface structures by Ar POA is mainly arisen not at the oxide side but at the SiC side of the interface layer since the UPS measurement with smaller  $\theta_c$  is more surface-sensitive in general for amorphous material. The valence band offset  $\Delta E_v$  was evaluated from the deconvolution of valence band spectra. Also, the conduction band offset  $\Delta E_c$  was evaluated from the subtraction of  $\Delta E_v$  from  $E_g$  of the interface layer, as listed in Tab. 1. It is found that the band offsets in both the oxidation methods change remarkably by Ar POA.

We have performed C-V measurements for the samples prepared by the same ways as those used in this experiment, *i.e.* samples (a)-(d). The large  $\Delta V_{\text{fb}}^{\text{dyn}}$  was observed in the case of the sample (a) (dry+quenched).[8] While, such a shift was not observed after Ar POA though the net number of interface trapped charges per unit area  $N_{\text{it}}$  slightly increased. In the case of pyrogenic oxidation, such a shift was not observed at all and the value of  $N_{\text{it}}$  was very small. The results obtained from C-V

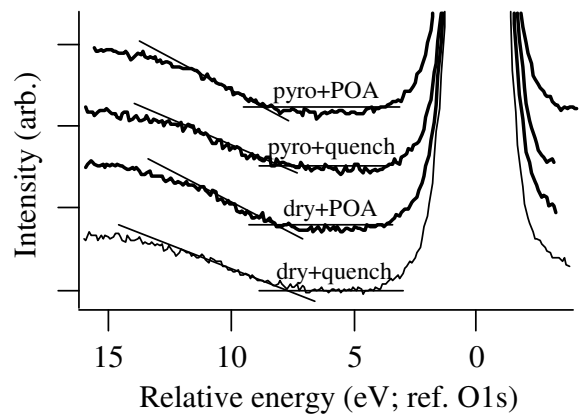


Fig. 2. O1s spectra of the samples (a)-(d).

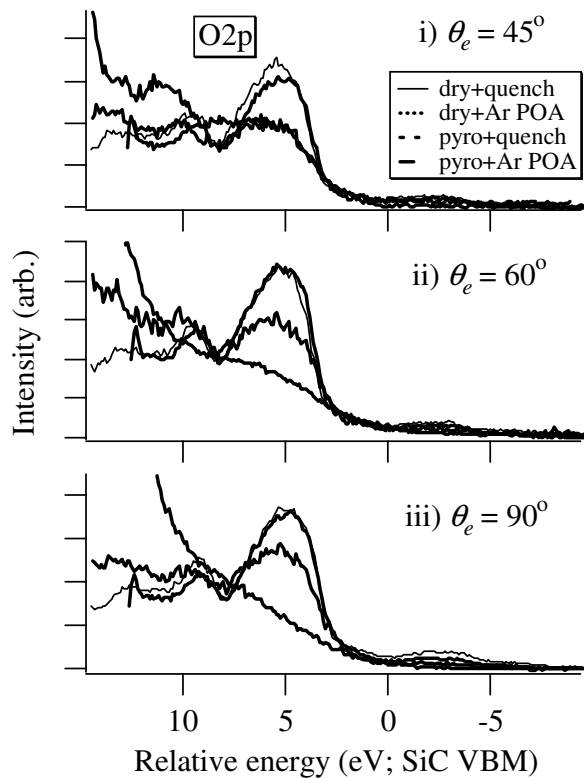


Fig. 3. UPS spectra of the samples (a)-(d) at various  $\theta_c$ .

measurements are also listed in Tab. 1. Compared between the cases of samples (a) with (c) and (b) with (d), it can be said that the sample having a low  $N_{it}$  has a large  $E_g$  value. However, in the relation between quenched and Ar POA samples, there is no correspondence. This disagreement results from the difference in the mechanism of the increase of  $E_g$  in the case of pyrogenic oxidations and Ar POA. The large  $V_{fb}$  and  $\Delta V_{fb}^{dyn}$  values observed in sample (a) correspond well with the small  $\Delta E_c$  and  $E_g$  values of the interface layer. The values of band offset change remarkably by Ar POA, while  $N_{it}$  increases a little. There is no correspondence between the value of  $Si^{1+}/Si^{0+}$  and any other experimental values.

The difference of pyrogenic oxidation from dry one is the existence of -H and -OH radicals. Therefore, a hydrogen-sensitive measurement should be carried out to clarify the hydrogen effects for the change of interface structure.

Table 1. Experimental results from XPS/UPS for samples (a)-(d), as well as those from C-V measurements.

	(a)dry+quench	(b)dry+POA	(c)pyro+quench	(d)pyro+POA
oxide thickness (nm)	1.35	1.47	1.13	1.47
$Si^{1+} / Si^{0+}$ ( $Si^{4+} / Si^{0+}$ )	0.37 (0.48)	0.29 (0.51)	0.25 (0.46)	0.34 (0.68)
$E_g$ of oxide (eV)	7.6	8.0	7.9	8.2
$\Delta E_v / \Delta E_c$ (eV)	3.8 / 0.8	2.7 / 2.4	3.8 / 1.1	3.0 / 2.6
$V_{fb} / \Delta V_{fb}^{dyn}$ (V)	16.5 / 10.8	3.5 / ~ 0	3.1 / 0.67	3.1 / ~ 0
$N_{it}$ (cm <sup>-2</sup> )	5.5X10 <sup>12</sup>	8.3X10 <sup>12</sup>	1.5X10 <sup>12</sup>	2.2X10 <sup>12</sup>

## Summary

We have studied the difference of oxide/SiC interface structures between dry and pyrogenic oxidation and the effect of Ar POA by XPS/UPS measurements. It is found from these studies, as well as those from C-V measurements, that there exist intermediate layers containing  $Si^{1+}$  oxidation states at the interfaces, and there is no correspondence between the thickness of the layer and the value from electrical measurements. It is also found that the valence band structure and the band-offset change remarkably by Ar POA in both cases of oxidation method.

## References

- [1] J.N. Shenoy, J.A. Cooper Jr., M.R. Melloch: IEEE Electron. Device Lett. Vol. 18 (1997), p.93.
- [2] V.V. Afanas'ev, M. Bassler, G. Pensl, M.J. Sculz: Phys. Stat. Sol. A Vol. 162 (1997), p.312.
- [3] L.A. Lipkin and J.W. Palmour: J. Electron. Mater. Vol. 25 (1996) p.909.
- [4] B. Hornetz, H.-J. Michel, and J. Halbritter: J. Mater. Res. Vol. 9 (1994), p.3088.
- [5] L.I. Johansson, C. Virojanadara, T. Eickhoff, and W. Drude: Surf. Sci. Vol. 529 (2003), p. 515.
- [6] Y. Hijikata, H. Yaguchi, M. Yoshikawa and S. Yoshida: Appl. Surf. Sci., Vol. 184/1-4 (2001), p.163.
- [7] Y. Hijikata, H. Yaguchi, M. Yoshikawa and S. Yoshida: Mater. Sci. Forum Vol. 389-393 (2002), p.1033.
- [8] M. Yoshikawa, Y. Hijikata et al.: Trans. IEICE C (in Japanese), J86-C (2003), p.426.
- [9] S. Miyazaki: J. Vac. Sci. Technol. B Vol. 19(6) (2001), p.2212.
- [10] M. Tabe, T. T. Chiang, I. Lindau and W. E. Spicer: Phys. Rev. B Vol. 34-4 (1986), p.2706.